NASA TM X- 66128

HELIUM IN THE TOPSIDE
VENUS IONOSPHERE

H. C. NTIS #3.00

J. R. HERMAN

NOVEMBER 1972

GSFC — GODDARD SPACE FLIGHT CENTER —
GREENBELT, MARYLAND

HELIUM IN THE TOPSIDE VENUS IONOSPHERE

by

J. R. Herman

Laboratory for Planetary Atmospheres
Goddard Space Flight Center
Greenbelt, Maryland 20771

HELIUM IN THE TOPSIDE VENUS IONOSPHERE

ABSTRACT

The quantity of helium in the Venus atmosphere can be estimated from an examination of the measured ionization profiles. The amount of helium necessary to give agreement between the computed and experimental results is approximately 4×10^8 cm^{-3} at 140 km. When an eddy diffusion coefficient of 10^6 cm^2 sec^{-1} is used, the atmospheric helium mixing ratio is found to be 6×10^{-5}; a value nearly ten times that for Earth.

HELIUM IN THE TOPSIDE VENUS IONOSPHERE

The best direct evidence for the presence of helium on Venus is obtained from the recent detection of its radioactive progenitors on the surface of Venus by Venera 8 (announced in Tass, 1972). Since the quantities of radioactive materials found were similar to measurements of Earth samples, the ultimate detection of helium on Venus should be a near certainty. Three years prior to the landing of Venera 8, Knudsen and Anderson (1969) assumed that the Venus helium production rate was similar to Earth's, but that the loss rate was due only to thermal escape (negligible relative to production), and calculated the helium atmospheric mixing ratio as 2×10^{-4}. Since this value is 40 times that for Earth, an attempt should be made to check for consistency with other data.

An additional measure of the helium content is afforded by the upper atmosphere and ionosphere measurements obtained from Mariner V. The Lyman α determination of the hydrogen density in the exosphere, Barth (1968), and the electron and total neutral density from the radio occultation experiment, Fjeldbo and Eshelman (1969), can be used in conjunction with atmospheric modeling to place limits on the helium concentration. The principal features of these measurements are: (1) An upper limit on the hydrogen density of 5×10^3 cm^{-3} at 500 km altitude; (2) the observed abrupt change in the electron density scale height in the vicinity of 200 km; (3) the value of the electron density above 250 km (about 10^4 cm^{-3}), and (4) the inferred neutral gas temperature in the isothermal region of about 650 °K.

A reference neutral atmosphere for this work can be constructed by selecting boundary values at 100 km altitude for each neutral species that are consistent with the known measurements. To produce the desired calculated atmosphere, the energy, momentum, and continuity equations are integrated for both the neutral and ionic species. The neutral atmosphere boundary conditions are adjusted to match the lower atmosphere measurements of total density and possible composition; approximately 97% CO_2 with up to 3% of minor constituents Ar, N_2, O_2, H_2, He, CO, and others, Marov (1972). Of these, the upper limits of N_2 and O_2 are about 2% and 0.1%, respectively. The remaining species are estimated at reference altitudes as shown in Table 1, and the complete atmospheric model in Figure 1.

TABLE 1

SPECIES	DENSITY (cm^{-3})	Reference Altitude (km)
N_2	5×10^{11} - 4×10^{12}	100
CO_2	2×10^{14} - 5×10^{14}	100
O_2	1×10^{10} - 2×10^{11}	100
He	0 - 2×10^{10}	100
H	$< 5 \times 10^3$	500
C	0 - 2×10^7	150
O	5×10^5 - 5×10^8	150
CO	1×10^9 - 1×10^{11}	100
N	5×10^5 - 5×10^8	150
NO	Unknown - $< 5 \times 10^6$	100

The value of the total density at 100 km altitude was chosen by extrapolating the lower atmospheric data taken by the Mariner and Venera spacecraft. Ainsworth and Herman (1972), and by requiring that the electron density reaches a maximum near an altitude of 145 km for Mariner conditions. The base temperature at 100 km was varied between 160 and 200°K, with 180°K adopted as a reference value. This temperature varia-tion is able to produce a shift in the peak altitude of the electron density of $\pm$ 5 km. Its effect on the He and He^+ distribution is small, and therefore a base temperature of 180°K is used throughout.

Since the purpose of this work is to discuss the effect of the varia-tion of neutral helium on the resulting electron density profile above 200 km, the appropriate equations and chemical reactions are summarized below. A one dimensional diffusion model is adopted using the continuity and momentum equations

$$\frac{\partial n_i}{\partial t} + \frac{\partial}{\partial z} (n_i v_i) = P_i - L_i n_i \tag{1}$$

$$\rho_i \frac{\partial v_i}{\partial t} = -\frac{\partial p_i}{\partial z} - \rho_i g + en_i E - \underset{\text{IONS}}{\sum_j K_{ij}(v_i - v_j)} - \underset{\text{NEUTRALS}}{\sum_j K_{ij} v_i} \tag{2}$$

where the higher order terms $\rho_i v_i \frac{\partial v_i}{\partial z}$, thermal diffusion, and the motion of the neutral atmosphere are neglected. The possibly unfamiliar symbols are $K_{ij} = n_i \mu_{ij} \nu_{ij}$, where μ_{ij} is the reduced mass and ν_{ij} is the collision frequency, Banks (1966), Dalgarno (1969), P_i is the total volume production

rate from both solar and chemical sources for the i th ionic species,
and $L_i n_i$ is the corresponding chemical loss rate. In the case of helium,
the total production of He^+ is from the solar EUV ionization of He com-
puted in the usual manner, Herman et al. (1971), based on the solar flux
given by Hinteregger (1970), and that arising from energetic secondary
photoelectrons. The chemical loss channels are described in Table 2.
The loss channels via atomic species all appear to have very small loss
rates, Fehsenfeld et al. (1966). It is that fact and the low measured
value of [H] that is mainly responsible for He^+ being the dominant top-
side ion. Much of the H^+ produced is lost by charge exchange with O at
a rate of 3.75×10^{-10} cm^{-3} sec^{-1} as well as by other rapid losses to
CO_2 and O_2, Banks (1972). Another possibility for a topside Venus ion
is C^+ since it is produced rapidly both by photoionization and charge
transfer processes, and is not lost at a large rate to other atomic
species. However, unless there are very large amounts of neutral carbon
present, its relatively heavy mass compared to He precludes it from a
significant contribution to the topside ions. Most of the C^+ that is pro-
duced is lost to CO_2 and O_2 with rates of 3.7×10^{-9} and 2.2×10^{-9} cm^{-3} sec^{-1}
respectively, McDaniel et al. (1970).

The result of using the above reaction rates, the appropriate photo-
ionization cross sections, Hinteregger (1965), McDaniel (1964), and
Sullivan and Holland (1964), and equations (1) and (2), yield the results
shown in Figure 2. The major ions adding up to the electron density
n_e are indicated in four altitude regimes. The bottomside is composed
mainly of CO_2^+, O_2^+, and NO^+. The relative amounts are governed

TABLE 2

Reaction	Rate	Reference
$H_e^+ + O_2 \rightarrow H_e + O + O^+$	1.5(-9)	Fehsenfeld (1966)
$H_e^+ + O_2 \rightarrow O_2^+ + H_e$	3.0(-10)	Warneck (1966)
$H_e^+ + CO_2 \rightarrow CO^+ + O + H_e$	9.6(-10)	Fehsenfeld (1966)
$\rightarrow O^+ + CO + H_e$	1.8(-10)	Fehsenfeld (1966)
$\rightarrow CO_2^+ + H_e$	6.0(-11)	Fehsenfeld (1966)
$H_e^+ + CO \rightarrow H_e + O + C^+$	1.7(-9)	Fehsenfeld (1966)
$H_e^+ + N_2 \rightarrow H_e + N + N^+$	7.1(-10)	Warneck (1966)
$\rightarrow H_e + N_2^+$	7.6(-10)	Warneck (1966)
$H_e^+ + e \rightarrow He + h\nu$	5.0(-12)	Biondi (1964)

by the amount of N and O present in the atmosphere. NO^+ is produced
copiously, even in the absence of NO, and can amount to half the total
ion density at the electron density maximum based on the limits of the
neutral atmosphere given in Table 1. As both N and O decrease with
altitude the amount of NO^+ also decreases rapidly giving way to O^+, CO_2^+,
and O_2^+. With further increases in altitude He^+ dominates all other
ions present.

The observations of n_e from Mariner V show a topside ion density
of about 10^4 cm^{-3} and a very abrupt slope change between the molecular
ion to the atomic ion region. Comparing the topside data to the results
in Figure 2 show that the measured profile falls between cases (b) and (c).

Accordingly, limits can be placed on the helium density above the tur-
bopause of from 3.5×10^8 to 5×10^8 at 140 km altitude. When an
eddy diffusion coefficient of $K = 10^6$ cm^2 sec^{-1} is used, the helium
density well below the turbopause if from 1×10^{10} to 1.5×10^{10} cm^{-3} at
100 km and leads to cases (b) and (c). This corresponds to a mixing
ratio of approximately 6×10^{-5}. The results obtained here, which in-
clude the effects of ion diffusion and self consistency with the tem-
perature calculation, require significantly more neutral helium than
previous estimates. Whitten (1970) obtained an estimate of about 0.1
of the present value from a dayside ionospheric calculation. McElroy
and Strobel (1969) estimated about 0.1 from a nightside calculation and
Knudsen and Anderson (1969) about 1/4. These factors are significant
because a reduction by a factor of 1/2 produces the results shown in
case (a) with a drastically decreased scale height and too small a value
of electron density. In the case of Whitten, enough approximations
were made in evaluating the terms in the momentum and continuity equations
that the accuracy of his results are difficult to evaluate. In particu-
lar, one of his key results is that the scale heights of CO^+ and O^+ are
the same as He^+. The results obtained from solving for each species shows
that CO^+ reaches a maximum of about 10^3 cm^{-3} at 250 km altitude where
the dominant ions are O_2^+, CO_2^+, O^+, and He^+ and decreases rapidly above
250 km, (CO^+ = 40 at 350 km). Similarly, O^+ reaches a maximum of about
8×10^3 at 260 km and decreases to about 1×10^3 at 360 km. The very
different He^+ scale height can be seen in Figure 2.

McElroy and Strobel (1969) estimated a mixing ratio of 10^{-4} by making an Earth analogy for the turbopause height. Since a lowering of the turbopause altitude (a strong function of total density) results in a lower requirement for the mixing ratio, the value estimates here, 6×10^{-5}, does not contradict their method of estimation.

The method employed here for determining where the cessation of turbulent mixing and the onset of diffusive separation occurs is based on the relative values of K_o and D, the eddy and binary diffusion coefficients, respectively. For altitudes where $K_o > D$, $K \simeq K_o$, and in the altitude range where $K_o \simeq D$ or $K_o < D$, K decreases rapidly so that the onset of diffusive separation takes place within about a 5 to 10 km range. This is verified experimentally for Earth, Keneshea and Zimmerman (1970) with the results approximated quite well by the form $K \simeq K_o \exp [-D/K_o]$. Expressing K in this manner permits their result to be scaled to the Venus atmosphere.

If, as McElroy and Strobel suggest, the nightside ionization above 200 km is to be maintained by lateral flow from the dayside, the amount of helium in the present model is sufficient. It should be noted that the nightside ionization ledge of 10^4 cm^3 below 200 km cannot be maintained by flow from the dayside because of the rapid $He^+ + CO_2$ charge exchange rate. In addition, if such a process were considered, it would require downward diffusion from higher altitudes. This He^+ flow in the presence of CO_2^+ ions would not be possible due to the presence of an upward electric field resulting from a $CO_2^+ - He^+$ mixture. Perhaps a combination of their suggestions, with the ionization ledge below

200 km produced by an influx of energetic solar wind particles, and with the topside produced by He^+ flow from the dayside would be appropriate.

In summary, the observed dayside ionization above 200 km can be satisfactorily accounted for with a helium density of about 4×10^8 cm^{-3} at 140 km altitude. This corresponds to a mixing ratio of 5×10^{-6} if the eddy diffusion coefficient is taken to be 10^6 cm^2 sec^{-1}. Such a model is consistent with estimates of helium generated from radioactive sources over geological time, and with the requirements for maintenance of the nightside ionosphere above 200 km by lateral flow of He^+ from the dayside of Venus.

REFERENCES

Ainsworth, J., and Herman, J. R., Analysis of the Venus Measurements, NASA/GSFC X-625-72-187 (1972).

Banks, P., Collision Frequencies and Energy Transfer: Ions, Planetary Space Sci., 14, 1105 (1966).

Banks, P., Difficulties with Thermal Protons in the Venusian Topside Ionosphere, J. Geophys. Res., 76, 8455 (1971).

Barth, C. A., Interpretation of the Mariner 5 Lyman Alpha Measurements, J. Atmospheric Sci., 25, 564 (1968).

Biondi, M. A., Electron-ion and Ion-Ion Recombination, Annales Geophys., 20, 5 (1964).

Dalgarno, A., Inelastic Collisions at Low Energies, Canadian J. of Chemistry, 47, 1723 (1969).

Fehsenfeld, F. C., Schmeltekopf, A. L., Golden, P. D., Schiff, H. I., and Ferguson, E. E., Thermal Energy Ion - Neutral Reaction Rates I. Some Reactions of Helium Ions, J. Chemical Phys., 44, 4087 (1966).

Fjeldbo, G., and Eshleman, V. R., Atmospheres of Venus as Studied with the Mariner 5 Dual Radio Frequency Occultation Experiment, Radio Science, 4, 879 (1969).

Herman, J. R., Hartle, R. E., and Bauer, S. J., The Dayside Ionosphere of Venus, Planet. Space Sci., 19, 443 (1971).

Hinteregger, H. E., Hall, L. A., and Schmidtke, G., Solar XUV Radiation and Neutral Particle Distribution in July 1963 Thermosphere, Space Research V, 1175 (1965).

Hinteregger, H. E., The Extreme Ultraviolet Solar Spectrum and its Variation During a Solar Cycle, Annales Geophys., 26, 547 (1970).

Keneshea, T. J., and Zimmerman, S. P., The Effect of Mixing Upon Atomic and Molecular Oxygen in the 70 to 170 km Region of the Atmosphere, J. Atmospheric Sci., 27, 831 (1970).

Knudsen, W.C. and Anderson, A.D., Estimate of Radiogenic He^4 and Ar^{20} Concentration in the Cytherean Atmosphere, J. Geophys. Res., 74, 5629 (1969)

McDaniel, E.W., Collision Phenomenon in Ionized Gases, John Wiley, New York (1964)

McDaniel, E.W., Cermak, V., Dalgarno, A., Ferguson,E.E., and Friedman, L., Ion Molecule Reactions, Wiley-Interscience, John Wiley, New York (1970)

Mcelroy, M.B., and Strobel, D.F., Models for the Nighttime Venus Ionosphere, J. Geophys. Res., 74, 1118 (1969)

Sullivan, J.O., and Holland, A.C., A Congeries of Absorption Cross Sections for Wavelengths less than 3000 A. II, AFAL Technical Report 65-228 (1964)

Warneck,P., Ion-Molecule Reaction Rates in an Oxygen Nitrogen Atmosphere, GCA Technical Report 66-13-N (1966). See also Schmeltkopf et al., J. Chem. Phys., 48, 2966 (1968)

Whitten, R.C., The Daytime Upper Ionosphere of Venus, J. Geophys. Res., 75, 3707 (1970)

FIGURE CAPTIONS

Figure 1: A model of the Venus neutral atmosphere above 100 km altitude.
Dashed lines refer to the upper scale and solid lines to
the lower scale. Thick lines are molecular species and thin
lines are atomic species. The boundary values are based on
Table 1, and for all but CO_2 and H are upper limits esti-
mated from lower atmospheric measurements or from chemical
equilibrium.

Figure 2: The calculated Venus ionosphere showing the major ions in
their respective regions of dominance. The topside iono-
sphere is shown for four cases of helium density based on
boundary values at 100 km. Solid lines are the electron
density and the dashed lines are the He^+ density. Two
cases are shown for the bottomside electron density for two
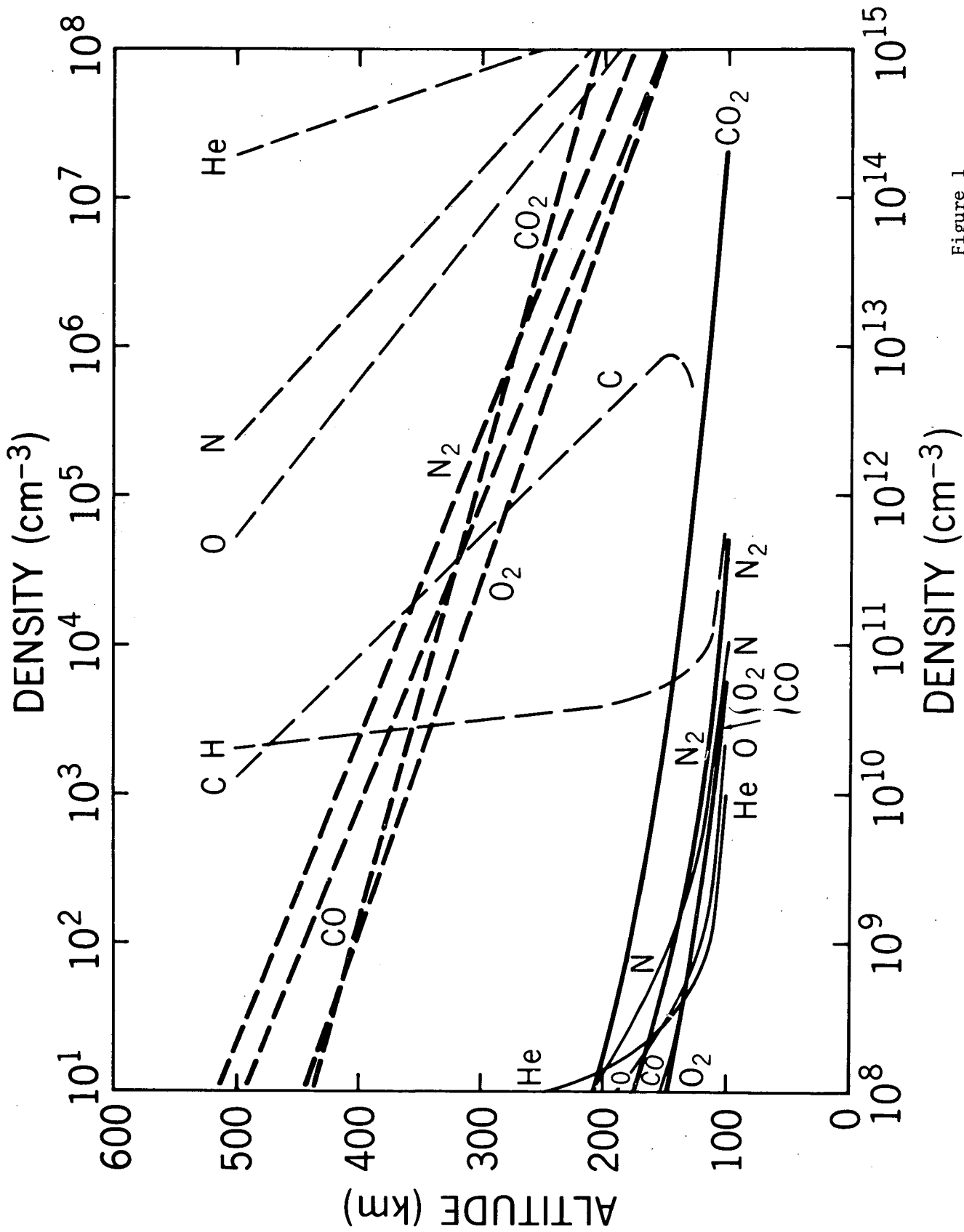different neutral gas temperatures T = 160°K and T = 180°K
at 100 km.

Figure 1

CASE [He] at 100 km

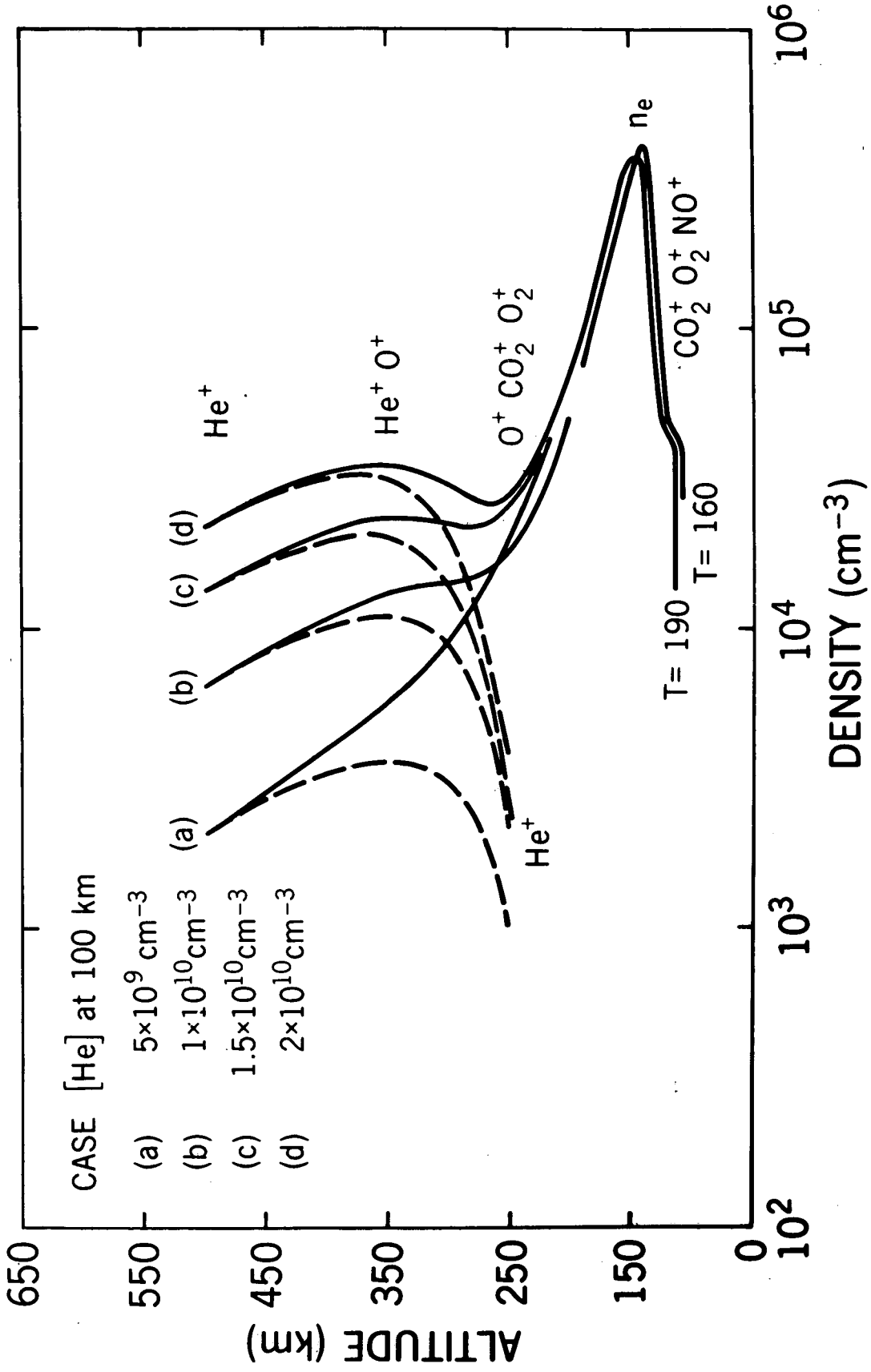| CASE	[He]
(a)	5×10^9 cm^{-3}
(b)	1×10^{10} cm^{-3}
(c)	1.5×10^{10} cm^{-3}
(d)	2×10^{10} cm^{-3}

He^+

He^+ O^+

O^+ CO_2^+ O_2^+

n_e

CO_2^+ O_2^+ NO^+

He^+

$T = 190$

$T = 160$

ALTITUDE (km)

650 550 450 350 250 150 0

DENSITY (cm^{-3})

10^2 10^3 10^4 10^5 10^6

Figure 2

NASA–GSFC